Filtered Multitone Multicarrier Modulation with Partially Overlapping Sub-Channels

Kai Shao, Luping Pi
Chongqing University of Posts and Telecomm
Chongqing, China
Email: shaokai@cqupt.edu.cn, piluping5@gmail.com

Juha Yli-Kaakinen, Markku Renfors
Tampere University of Technology
Tampere, Finland
Email: juha.yli-kaakinen@tut.fi, markku.renfors@tut.fi

***Abstract*—Future wireless networks demand multicarrier modulation schemes with improved spectrum efficiency and superior spectrum containment. Orthogonal frequency division multiplexing (OFDM) has been the favorite technique in recent developments, but due to its limited spectrum containment, various alternative schemes are under consideration for future systems. Theoretically, it is not possible to reach maximum spectrum efficiency, high spectral containment, and orthogonality of subcarriers simultaneously, when using quadrature amplitude modulation (QAM) for subcarriers. This has motivated the study of non-orthogonal multicarrier modulation schemes. This paper focuses on the filtered multitone (FMT) scheme, one of the classical configurations of filter bank multicarrier (FBMC) modulation utilizing QAM subcarrier symbols. Our main aim is to improve the spectral efficiency of FMT by introducing controlled overlap of adjacent subchannels. An analytical model is developed for evaluating the tradeoffs between spectrum efficiency and intercarrier interference (ICI) introduced by the overlap. An efficient fast convolution waveform processing scheme is adopted for the generation of the proposed waveform. It allows effective adjustment of the roll-off and subcarrier spacing to facilitate waveform adaptation in real time. Analytical studies, confirmed by simulation results, indicate that the proposed FMT system can obtain significant spectral density improvement without requiring additional ICI cancellation techniques.**

I. Introduction

The future cellular communication system generations are expected to support, in a unified framework, a wide scale of services, such as enhanced mobile broadband (eMBB) with Gbps data rates, massive machine type communications (mMTC), as well as ultra-reliable and low latency machine type communications (URRLC) [1]. There is a widespread agreement that such an ambitious goal will be realized in a combination of asynchronous heterogeneous network scenarios, requiring the physical modulation schemes with several challenging elements, including superior spectrum containment, improved bandwidth efficiency, etc. The well-known cyclic prefixed orthogonal frequency division multiplexing (CP-OFDM) is not suitable for such co-existence scenarios, because its good performance is guaranteed only when synchronism and inter-subcarrier orthogonality are strictly maintained. Specifically, CP-OFDM has one major limitation, i.e., poor side-lobe confinement due to the use of rectangular pulse shape, which results in high out-of-band emissions (OBE) [2], [3]. The high level of spectral side lobes makes it necessary to have wide guardbands between asynchronous multiplexes, and OFDM sidelobe control has gained a lot of attention since early 2000's [4]. Recently, in the 5G context, this issue has gained more interest and the strong candidate waveforms include filtered OFDM schemes [5], [6], [3], [7].

An attractive alternative to CP-OFDM based schemes for the considered scenarios is the class of filter bank multicarrier (FBMC) modulation. A relatively widely studied filter bank based waveform is FBMC/OQAM (filter bank multicarrier/offset-QAM, also known as OFDM /OQAM) [8], [9]. FBMC/OQAM is characterized by overlapping subchannels with maximum density, lack of CP, and the need for offset-QAM subcarrier modulation to reach orthogonality. However the offset-QAM signal structure introduces various challenges regarding effective pilot schemes for synchronization and channel estimation, as well as certain multi-antenna configurations, especially Alamouti space-time coding.

QAM symbol transmission and maximum spectral efficiency are two crucial issues in future FBMC developments. One interesting recent proposal is a scheme named as filter-bank multicarrier-quadrature amplitude modulation (FBMC-QAM) [10], [11]. This proposal adopts two different prototype filters, different for the even and odd-indexed subcarriers, and performs the QAM transmission with maximum spectral efficiency. However, the subcarriers of FBMC-QAM do not maintain orthogonality. FBMC-QAM variants [12] have also been considered using common FBMC/OQAM prototype filters, like the PHYDYAS filter bank [13], which results in similar level of intercarrier interference (ICI).

Another well-known orthogonal FBMC scheme is filtered multitone (FMT) [14]. The main benefit of FMT, comparing with FBMC/OQAM, is that basic QAM modulation can be used in subcarriers, which allows more direct application of pilot based synchronization and channel estimation schemes, as well as multi-antenna configurations developed for CP-OFDM. On the other hand, an FMT system needs higher subcarrier spacing than OFDM or FBMC/OQAM. In other words, the orthogonality of an FMT is reached at the expense of sacrificing the spectral efficiency. FMT is using square-root raised-cosine (RRC) type Nyquist pulse shaping for subcarriers, and reducing the roll-off allows to reduce the subcarrier spacing, improving the spectrum efficiency. Howe-

This work was supported by the Academy of Finland under Project 284724.

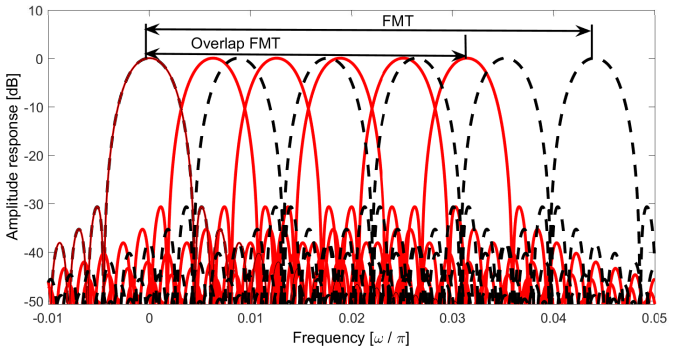

Fig. 1. Spectra of FMT and overlapping subchannel FMT using time-domain RRC-type filter of order 1024 and roll-off of 1. Six subchannels out of 256 are shown.

ver, small roll-off means high filter order, leading to increased complexity and long impulse response tails in transmission bursts.

In this paper we investigate possibilities to improve FMT's characteristics by allowing controlled amount of overlap between subchannels. This compromises the orthogonality but improves spectrum efficiency with reasonable values of roll-off and filter order. We present a flexible and effective scheme for implementing FMT with overlapping subchannels (O-FMT) based on the fast-convolution (FC) processing, which has recently been introduced in the waveform processing context [15], [16]. In Section II we develop an analytical model for ICI as a function of subchannel overlap and roll-off. The generation of O-FMT using FC filter bank is presented in Section III and Section IV gives the performance evaluation in terms of spectrum efficiency vs. interference level. Conclusions are included in Section V.

II. Intercarrier Interference Analysis

The main idea of O-FMT is compared with basic FMT in Fig. 1, where RRC filter with roll-off factor of 1 is used as the prototype filter. In O-FMT, the subcarrier spacing is reduced when compared to FMT with non-overlapping adjacent subchannels. The overlap of subcarriers introduces ICI. In this section, our target is to express the ICI analytically in terms of subcarrier spacing and roll-off.

The main parameters in the following analysis are defined as follows:

- β is the roll-off factor
- f_s is the sampling rate
- N is the subchannel oversampling factor
- $f_c = f_s/N$ is the subcarrier symbol rate
- $(1+\beta)f_c$ is the subcarrier spacing in FMT
- $(1+\beta)f_c - \Delta f$ is the subcarrier spacing in O-FMT
- $\omega_c = 2\pi/N$ and $\Delta\omega = 2\pi\Delta f$ are the normalized angular frequencies corresponding to f_c and Δf.

The amplitude response of the prototype RRC filter (DC subchannel) can be expressed as

$$H_{RRC}(\omega) = \begin{cases} B, & |\omega| < \omega_1 \\ \frac{B}{\sqrt{2}}\sqrt{1+\cos(\pi\frac{|\omega|-\omega_1}{\beta\omega_c})}, & \omega_1 \le |\omega| \le \omega_2 \\ 0, & |\omega| > \omega_2 \end{cases} \quad (1)$$

where $\omega_1 = \frac{1-\beta}{2}\omega_c$ and $\omega_2 = \frac{1+\beta}{2}\omega_c$ are the passband and stopband edges of the DC subchannel and $B = \sqrt{2\pi/\omega_c}$.

Let us then analyze the crosstalk between subcarriers in O-FMT. Without loss of generality, we can consider the overlapping part of subchannels 0 and 1, with center frequencies at 0 and $(1+\beta)\omega_c - \Delta\omega = 2\omega_2 - \Delta\omega$. The overlapping region has left and right edges at $\omega_L = \omega_2 - \Delta\omega$ and $\omega_R = \omega_2$, respectively. In this region, the RRC frequency responses of subchannels 0 and 1 can be expressed as

$$\begin{aligned} H_L(\omega) &= \frac{B}{\sqrt{2}}\sqrt{1+\cos(\pi\frac{\omega-\omega_1}{\beta\omega_c})} \\ H_R(\omega) &= \frac{B}{\sqrt{2}}\sqrt{1+\cos(\pi\frac{2\omega_2-\Delta\omega-\omega-\omega_1}{\beta\omega_c})}. \end{aligned} \quad (2)$$

In the absence of channel attenuation and frequency selectivity, the received subcarrier power is given by $S = B^4/4$ and the interference power can be evaluated as

$$\begin{aligned} P_i &= \int_{\omega_L}^{\omega_R} H_L^2(\omega)H_R^2(\omega)\,d\omega \\ &= \frac{B^4}{4}\int_{\omega_L}^{\omega_R}(1+\cos(\pi\frac{\omega-\omega_1}{\beta\omega_c})) \\ &\quad \cdot(1+\cos(\pi\frac{2\omega_2-\Delta\omega-\omega-\omega_1}{\beta\omega_c}))\,d\omega. \end{aligned} \quad (3)$$

Starting from a simplified form of the integrand, it can be developed as follows:

$$\begin{aligned} I &= (1+\cos(x))(1+\cos(y)) \\ &= 1+\cos(x)+\cos(y)+\cos(x)\cos(y) \\ &= 1+2\cos(\frac{x+y}{2})\cos(\frac{x-y}{2})+\frac{\cos(x+y)}{2}+\frac{\cos(x-y)}{2} \end{aligned} \quad (4)$$

Since $\omega_2 - \omega_1 = \beta\omega_c$, we can write:

$$\begin{aligned} x+y &= \frac{\pi}{\beta\omega_c}(\omega-\omega_1+2\omega_2-\Delta\omega-\omega-\omega_1) \\ &= 2\pi+\frac{2\pi}{\beta\omega_c}\frac{\Delta\omega}{2} \\ x-y &= \frac{\pi}{\beta\omega_c}(\omega-\omega_1-2\omega_2+\Delta\omega+\omega+\omega_1) \\ &= \frac{2\pi}{\beta\omega_c}(\omega-\omega_2-\frac{\Delta\omega}{2}) \end{aligned} \quad (5)$$

Now the normalized interference power can be developed

further as follows:

$$P_i/S = \int_{\omega_L}^{\omega_R} \Big(1 + \frac{1}{2}\cos(\frac{\pi\Delta\omega}{\beta\omega_c}) + \frac{1}{2}\cos(\frac{2\pi}{\beta\omega_c}(\omega - \omega_2 + \frac{\Delta\omega}{2})) + 2\cos(\pi + \frac{\pi\Delta\omega}{2\beta\omega_c})\cos\big(\frac{\pi}{\beta\omega_c}(\omega - \omega_2 - \frac{\Delta\omega}{2})\big)\Big)\, d\omega. \quad (6)$$

Finally, the integration gives:

$$P_i/S = \big(1 + \frac{1}{2}\cos(\frac{\pi\Delta\omega}{\beta\omega_c})\big)\Delta\omega + \frac{\beta\omega_c}{2\pi}\sin(\frac{\pi\Delta\omega}{\beta\omega_c}) - \frac{4\beta\omega_c}{\pi}\cos(\frac{\pi\Delta\omega}{2\beta\omega_c})\sin(\frac{\pi\Delta\omega}{2\beta\omega_c}). \quad (7)$$

This expression gives the power leakage between adjacent subcarriers. Most of the subcarriers receive interference from both sides. Therefore, the signal-to-interference ratio (SIR) of edge subcarriers is S/P_i and the SIR of other subcarriers is $S/(2P_i)$.

III. Generation of Overlapping FMT

Our target is to develop a dynamic O-FMT system, where the roll-off and subcarrier spacing can be adjusted in real-time based on user requirements, network load, and interference scenario. However, it is quite complicated to implement such a scheme using the traditional time-domain polyphase filter bank techniques, even for simulation based testing of the idea. This paper uses a special implementation scheme for multirate filters and filter banks which is based on fast-convolution (FC) processing [15], [16], [17]. The main idea of FC is that a high-order filter can be implemented effectively through multiplication in frequency-domain, after taking DFTs of the input sequence and the filter impulse response. In practice, efficient implementation techniques, like FFT/IFFT, are used for the transforms, and overlap-save processing is applied for processing long sequences. The application of FC to multicarrier waveform processing was presented in [16], and the authors have introduced the idea of FC-implementation of FMT systems in [17] as well.

One very important feature of the FC structure in this context is that the RRC-type sub-channel filters can be constructed in FFT-domain in a flexible way. This is based on using fixed transition band weights for different subchannel bandwidths. The weight mask can be obtained readily by frequency sampling the transition band of the RRC function. The overall frequency-domain weight mask consist of two symmetric transition bands, 1-valued passband, and 0-valued stopband. Using a single prototype transition band, the roll-off factor of each subchannel can be tuned by adjusting the passband width. For 2x-oversampled subchannel signals, the short transform length in FC processing should be twice the 3 dB bandwidth. This is achived by having $2p+1$ ones in the passband, $p+1$ zeros in the lower stopband and p zeros in the upper stopband. If t is the number of non-trivial transition band weights on both sides, then the roll-off factor can be expressed as $\beta = \frac{t+1}{p+t+1}$. Fig. 2 shows four examples with $p = \{0, 2, 8, 24\}$ and $t = 7$, leading to roll-off factors of $\beta = \{1, 0.8, 0.5, 0.25\}$, respectively.

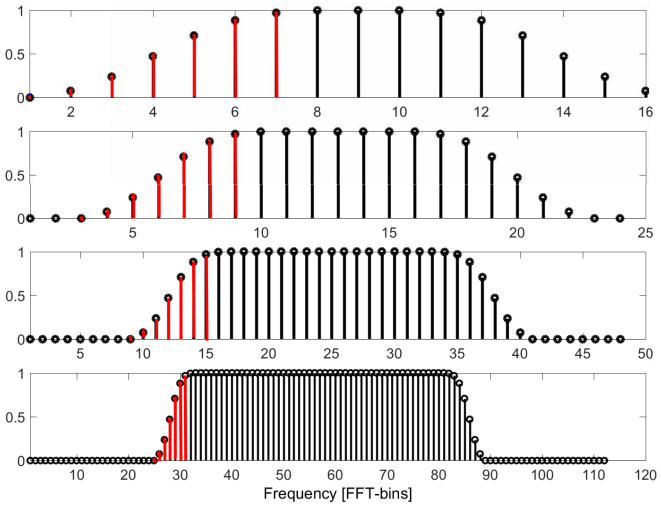

Fig. 2. Subchannel weight masks for $\beta = \{1,\ 0.8,\ 0.5,\ 0.25\}$ and $t = 7$ transition band weights. Basic weight mask is highlighted.

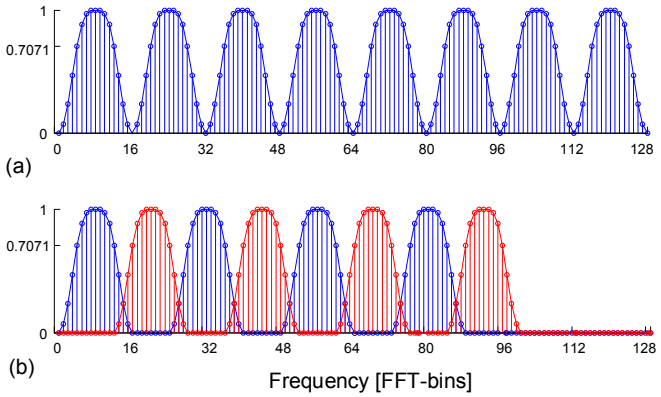

Fig. 3. Examples of subchannel configurations for FMT and O-FMT.

The other interesting feature of FC processing is the flexibility of subcarrier spacing, since all operations are performed in the FFT-domain. Fig. 3 shows two examples, one with non-overlapping subchannels, another one with the overlap of three FFT bins between adjacent subchannels. The only difference is the center frequency setting of each subchannel, which can be dynamically adjusted in FC-based implementation.

Frequency sampling of the RRC function is a straightforward way to design the subchannel filters for O-FMT. However, using the optimization methods presented in [16], it possible to enhance the performance of RRC-type filters for FMT. This has an effect on the inband interference within each subcarrier and ICI between subcarriers. In basic (non-overlapping) FMT, these interference effects are primarily due to circular distortion appearing with smaller overlapping

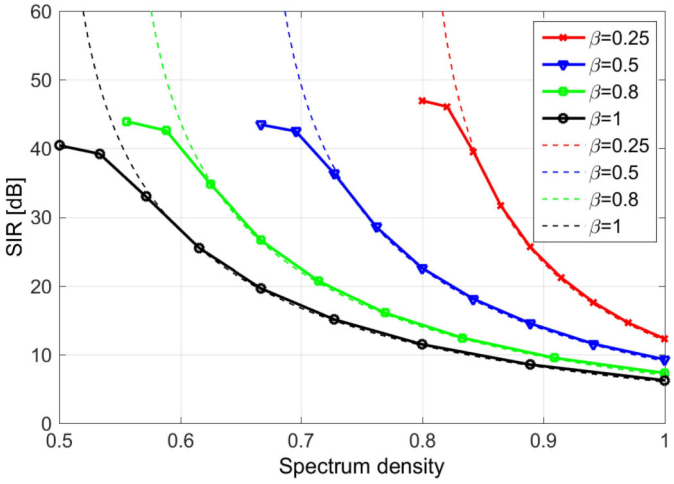

Fig. 4. Analytical and simulation based SIR performance for O-FMT with different roll-offs and subchannel overlaps. For the simulation case, frequency-sampled RRC design is used.

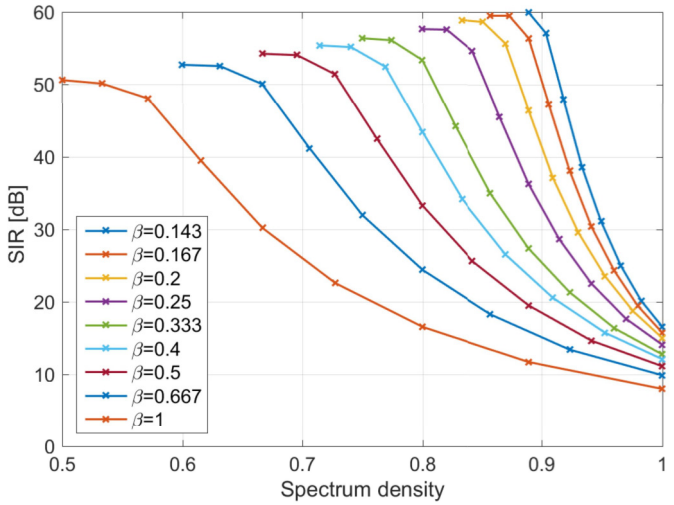

Fig. 5. Simulation based SIR performance for O-FMT with different roll-offs and subchannel overlaps using optimized weight mask. The markers indicate the subchannel overlap, ranging from 0 to 8 FFT bins, from left to right, respectively.

factors in FC processing. The examples of the following section demonstrate that the filter optimization has also a positive effect on the performance of O-FMT.

IV. Performance Evaluation

Fig. 4 compares the analytical SIR performance derived in Section II with simulation results in a case where the long FFT length of FC is 1024, the transition bands consist of $t = 7$ non-trivial weights, and the roll-off factors of $\beta = \{1, 0.8, 0.5, 0.2\}$ are used. Here the simulation model uses transition band weights which are derived from the RRC function by frequency sampling. The 'Spectrum density' on the horizontal axis is defined as the inverse of the normalized subcarrier spacing. In the non-overlapping FMT cases, this

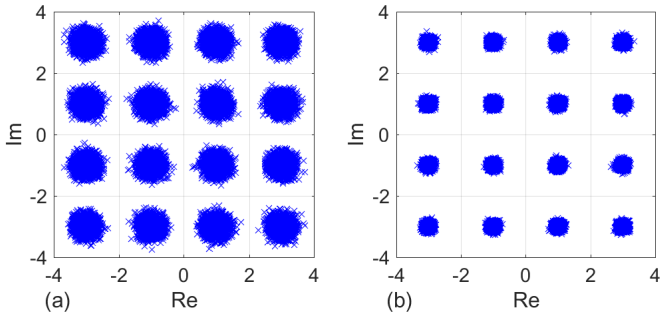

Fig. 6. Scatter diagram for O-FMT with 16-QAM modulation, $\beta = 0.2$, and 5-bin overlap. (a) Frequency-sampled RRC design. (b) Optimized design.

takes the value of $\frac{1}{1+\beta}$. We can see very good match between analytical and simulation results in the range where the SIR is below 40 dB. Beyond this range, when there is no subchannel overlap, the circular distortion in FC processing with the used overlap of 0.5 dominates the interference. Fig. 5 shows the simulated performance with optimized filter weight coefficients, with wider set of roll-off factors, while the configuration is otherwise the same as in Fig. 4. We can see that the circular interference level is significantly reduced and, remarkably, the interference due to subchannel overlap is reduced as well.

Based on Fig. 5, we can evaluate the spectrum density with reasonable interference levels. This depends on the used subcarrier modulation order, and the acceptable SIR level can be based on the error vector magnitude (EVM) specifications of the LTE system. For QPSK modulation the maximum EVM is 17.5%, corresponding to 15 dB SIR. Taking a 3 dB safety margin, we check different combinations of roll-off and overlap reaching 18 dB SIR. This is reached with $\beta = 0.5$ and subchannel overlap of 6 FFT bins, and the resulting spectrum density is 0.89. As an other alternative, with $\beta = 0.2$ and overlap of 7 FFT bins, the resulting spectrum density is 0.975. For 16-QAM modulation, the maximum EVM is 22 dB (8%) and 25 dB SIR is reached, e.g., with $\beta = 0.5$ and overlap of 5 FFT bins or $\beta = 0.2$ and overlap of 5 FFT bins, giving spectrum densities of 0.84 and 0.93, respectively. In non-overlapping FMT, the corresponding spectral densities with $\beta = 0.5$ and $\beta = 0.2$ are 0.67 and 0.83, respectively, so we can see that significant increase in spectrum efficiency can be reached by O-FMT, e.g., 33% with QPSK and $\beta = 0.5$ and 15% with QPSK and $\beta = 0.2$. Fig. 6 shows the scatter diagram for the O-FMT case with 16-QAM modulation, $\beta = 0.2$, and 5-bin overlap, for both filter designs. This demonstrates again that the optimized filter design helps to reduce the interference significantly.

With the used transition bandwidth of 8 FFT bins, the resulting subchannel bandwidths with $\beta = 0.5$ and $\beta = 0.2$ are 24 and 48 FFT bins, respectively. Reducing the relative transition bandwidth increases the circular distortion effects and requires the use of higher overlap. Depending mainly on the used modulation order, transition bandwidths of 4 or 5 FFT bins may be possible, resulting in proportional decrease

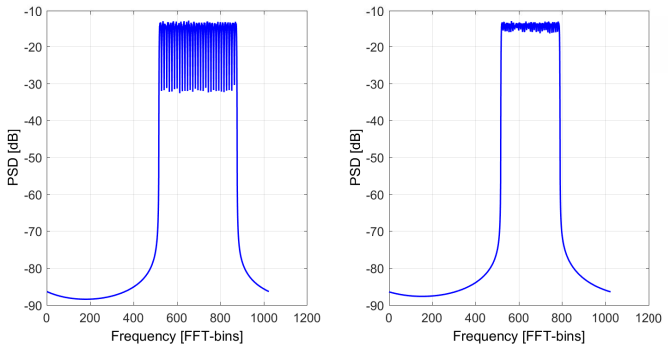

Fig. 7. PSD comparison between normal FMT (left) and O-FMT (right) in QPSK modulation case with $\beta = 0.5$ and overlap of 6 FFT bins in the O-FMT case.

in the subchannel bandwidths.

Finally, Fig. 7 compares the power spectral density (PSD) between normal FMT and O-FMT with QPSK subcarrier modulation, roll-off factor of 0.5, 30 subcarriers, and overlap of 6 FFT bins in the O-FMT case. The proposed O-FMT has similar out-of-band emissions compared to the normal FMT, however, the occupied spectral width is reduced by 25% in O-FMT.

V. Conclusion

It was demonstrated that the fast-convolution filter bank approach provides an effective and flexible way for implementing overlapping FMT systems with adjustable roll-off and adjustable subchannel overlap. FC-FB is used for waveform processing both on the transmitter and receiver sides, and it supports also effective subchannel equalization [18].

An accurate analytical model was developed for the ICI produced by subchannel overlap. Here it was applied for FC weight masks obtained through frequency sampling the RRC function, but the same approach can be applied for any subchannel filter design. The subchannel filter weight mask optimization was found to give significantly reduced interference due to overlap, in addition to relaxing the effects of circular distortion due to finite overlap in FC processing. Numerical results demonstrated 15% to 30% increased spectrum density for O-FMT, compared to basic FMT, depending on the modulation order and roll-off.

FC-FB based O-FMT allows effective adjustment of the roll-off and subcarrier spacing to facilitate waveform adaptation in real time depending on the targeted modulation and coding scheme (MCS). It is also possible to use simultaneously different numerologies (regrading subchannel bandwidth, roll-off, and subchannel overlap) for different users' groups of subcarriers. Also FC-FB based implementations have been found to be more efficient than polyphase filter banks for FMT (and also for FBMC/OQAM) in terms multiplication rate as a basic computational complexity metric [17].

Preliminary studies indicate that the peak-to-average power ratio (PAPR) characteristics of O-FMT are quite similar to those of OFDM and FBMC/OQAM with the same number of subcarriers.

References

[1] A. Shafi, A.F. Molisch, P.J. Smith, T. Haustein, P. Zhu, P.D. Silva, F. Tufvesson, A. Benjebbour, G. Wunder, "5G: A tutorial overview of standards, trials, challenges, deployment and practice," *IEEE Journal on Selected Areas in Communications*, vol. 35, pp. 1201-1221, June 2017.

[2] P. Banelli, S. Buzzi, G. Colavolpe, A. Modenini, F. Rusek, A. Ugolini, "Modulation formats and waveforms for 5G networks: Who will be the heir of OFDM? An overview of alternative modulation schemes for improved spectral efficiency," *IEEE Signal Processing Mag.*, vol. 31, pp. 80-93, June 2014.

[3] R. Gerzaguet et al., "The 5G candidate waveform race: A comparison of complexity and performance," *EURASIP Journal on Wireless Communications and Networking*, 2017, DOI 10.1186/s13638-016-0792-0

[4] A. Loulou and M. Renfors, "Enhanced OFDM for fragmented spectrum use in 5G systems," *Transactions on Emerging Telecommunications Technologies*, vol. 26, no. 1, pp. 31-45, 2015.

[5] V. Vakilian, T. Wild, F. Schaich, S. ten Brink, and J. F. Frigon, "Universal-filtered multi-carrier technique for wireless systems beyond LTE," *2013 IEEE Globecom Workshops*, Atlanta, GA, pp. 223-228, Dec. 2013.

[6] J. Abdoli, M. Jia, and J. Ma, "Filtered OFDM: A new waveform for future wireless systems," in *Proc. 2015 IEEE 16th International Workshop on Signal Processing Advances in Wireless Communications (SPAWC)"*, Stockholm, Sweden, pp. 66-70, June 2015.

[7] J. Yli-Kaakinen, T. Levanen, S. Valkonen, K. Pajukoski, J. Pirskanen, M. Renfors, and. M. Valkama, "Efficient fast-convolution-based waveform processing for 5G physical layer," in *IEEE Journal on Selected Areas in Communications*, vol. 35, no. 6, pp. 1309-1326, June 2017.

[8] P. Siohan, C. Siclet, and N. Lacaille, Analysis and design of OFDM/OQAM systems based on filterbank theory, *IEEE Trans. Signal Process.*, vol. 50, no. 5, pp. 1170-1183, May 2002.

[9] B. Farhang-Boroujeny and R. Kempter, "Multicarrier communication techniques for spectrum sensing and communication in cognitive radios," *IEEE Communications Magazine*, vol. 46, no. 4, pp. 80-85, April 2008.

[10] Y. H. Yun, C. Kim, K. Kim, Z. Ho, B. Lee, and J.-Y. Seol, "A new waveform enabling enhanced QAM-FBMC systems," in *Proc. IEEE International Workshop on Signal Processing Advances in Wireless Communications (SPAWC)*, Stockholm, Sweden, June 2015.

[11] H. Nam, M. Choi, S. Han, C. Kim, S. Choi, D. Hong, "A new filter-bank multicarrier system with two prototype filters for QAM symbols transmission and reception," *IEEE Trans. on Wireless Communications*, vol. 15, no. 9, pp. 5998-6009, Sept. 2016.

[12] R. Zakaria and D. Le Ruyet, "On maximum likelihood MIMO detection in QAM-FBMC systems," in *Proc. IEEE International Symposium on Personal, Indoor, and Mobile Radio Communications (PIMRC)*, Istanbul, Turkey, Sept. 2010.

[13] M. Bellanger et al. "FBMC physical layer: A primer," 2010, http://www.ict-phydyas.org/

[14] G. Cherubini, E. Eleftheriou, S. Oker, and J. M. Cioffi, "Filter bank modulation techniques for very high speed digital subscriber lines," *IEEE Communications Magazine*, vol. 38, no. 5, pp. 98-104, May 2000.

[15] J. Yli-Kaakinen and M. Renfors, "Fast-convolution filter bank approach for non-contiguous spectrum use," in *Proc. Future Network and Mobile Summit*, Lisbon. Portugal, pp. 1-10, June 2013.

[16] M. Renfors, J. Yli-Kaakinen, and F. J. Harris, "Analysis and Design of Efficient and Flexible Fast-Convolution Based Multirate Filter Banks," *IEEE Transactions on Signal Processing*, vol. 62, no. 15, pp. 3768-3783, Aug.1, 2014.

[17] K. Shao, J. Alhava, J. Yli-Kaakinen, and M. Renfors, "Fast-convolution implementation of filter bank multicarrier waveform processing," in *Proc. IEEE Int. Symp. on Circuits and Systems (ISCAS)*, Lisbon, Portugal, pp. 978-981, May 2015.

[18] M. Renfors and J. Yli-Kaakinen, "Channel equalization in fast-convolution filter bank based receivers for professional mobile radio," in *Proc. European Wireless*, Barcelona, Spain, May 2014.